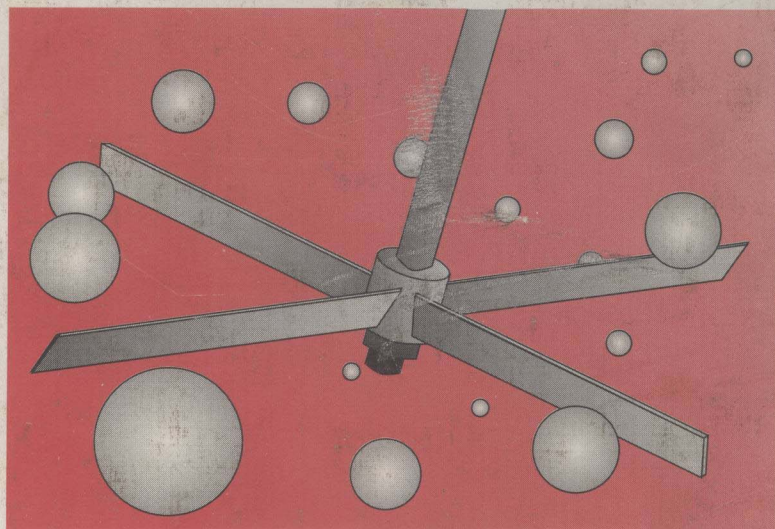


# PROCESS MIXING: Chemical and Biochemical Applications

---

*Gary B. Tatterson and Richard V. Calabrese, Volume editors*





# Process Mixing:

## Chemical and Biochemical Applications

A publication of the North American Mixing Forum (NAMF) of the AIChE

*Elmer L. Gaden, Jr., series editor*

*Gary B. Tatterson and Richard V. Calabrese,  
volume editors*

Acharya, N.  
Bertrand, F.  
Bodemeier, S.  
Bowe, M.J.  
Brodkey, Robert S.  
Broring, S.  
Chang, H.-C.  
Choplin, L.  
Claas, W.  
de la Fuente, E. Brito  
Detrez, Claude  
Detsch, R.M.  
Diekmann, Timothy J.  
El-Hamouz, A.M.  
Erickson, L.E.  
Falk, Laurent  
Fasano, Julian B.  
Fischer, J.  
Ford, L.H.  
Forney, L.J.

Forschner, Peter  
Fournier, Marie-Christine  
Fox, Rodney O.  
Glasgow, Larry A.  
Gwilliam, George  
Haam, Seung Joo  
Hanley, T.R.  
Hoffman, Peter D.  
Hua, Jiaming  
Kaplan, Len  
Krebs, Rainer  
Lacroix, R.  
Leuliet, J.C.  
Lin, Wei  
Long, Richard T.  
Lubbart, A.  
Mann, R.  
Muralidhar, R.  
Neogi, Swati  
Oldshue, J.Y.

Perez, Ramon  
Pierce, David A.  
Ramkrishna, R.  
Reimus, Paul  
Renno, Gerd  
Sampson, Kendree J.  
Satija, Sunil  
Schneider, Torsten  
Sen, M.  
Sharma, R.N.  
Siddiqui, Habib  
Smith, Gene  
Stairmand, J.W.  
Stone, Teresa  
Suihla, C. Kurt  
Tanguy, P.A.  
Tavarez, Israel  
Tobin, T.  
Villermoux, Jacques  
Yiin, Tian-yih  
Zhang, Guotai

### AIChE Staff

Maura Mullen, Managing Editor; Thomas E.H. Campbell, editorial assistant

Inquiries regarding the publication of Symposium Series Volumes should be directed to

**Dr. Elmer L. Gaden, Jr., series editor,  
University of Virginia, Department of Chemical Engineering,  
Thornton Hall, Charlottesville, Virginia 22903-2442. FAX (804) 924-6270.**

Number 286

AIChE Symposium Series  
1992

Volume 88

*Published by*  
American Institute of Chemical Engineers

345 East 47 Street

New York, New York 10017

Copyright 1992

American Institute of Chemical Engineers  
345 East 47 Street, New York, N.Y. 10017

*AICHE shall not be responsible for statements or opinions  
advanced in papers or printed in its publications.*

**Library of Congress Cataloging-in-Publication Data**

Process mixing: chemical and biochemical applications / Gary  
B. Tatterson and Richard Calabrese, editors.

p. cm. — (AIChE symposium series ; no. 286, v. 88)

“First official publication of the North American Mixing  
Forum” — Foreword.

Includes index.

ISBN 0-8169-0566-5 (alk. paper)

1. Mixing—Congresses. I. Tatterson, Gary B. II. Calabrese, Richard,  
1946– . III. American Institute of Chemical Engineers. IV. Series:  
AIChE symposium series ; no. 286.

TP156.M5P76 1992

660'.284292—dc20

92-8353

CIP

Authorization to photocopy items for internal or personal use, or the internal or personal use of specific clients, is granted by AIChE for libraries and other users registered with the Copyright Clearance Center (CCC) Transactional Reporting Service, provided that the \$2.00 fee per copy is paid directly to CCC, 21 Congress St., Salem, MA 01970. This consent does not extend to copying for general distribution, for advertising, or promotional purposes, for inclusion in a publication, or for resale.

Articles published before 1978 are subject to the same copyright conditions and the fee is \$3.50 for each article. AIChE Symposium Series fee code: 0065-8812/92 \$3.50.

## FOREWORD

Mixing is part of the infrastructure of the chemical, petrochemical and biochemical industries. However, concerns have been raised that these industries are in need of better characterization of mixing, mass transfer, reaction, multiphase fluid mixing, etc, because of economic significance of mixing.

Mixing problems arise in both the design of new equipment and in the retrofitting of new processes into existing equipment. Research advances in mixing will significantly affect the success of emerging technologies and the efficient use of natural resources as well as contribute to safety and environmental quality.

It is with this purpose that this symposium was developed.

This symposium is the first official publication of the North American Mixing Forum (NAMF) of the AIChE. The North American Mixing Forum was officially recognized as part of the American Institute of Chemical Engineers in 1991.

Gary B. Tatterson  
Department of Chemical Engineering  
North Carolina A&T State University  
Greensboro, NC 27411

Richard V. Calabrese  
Department of Chemical Engineering  
University of Maryland  
College Park, MD 20742

#### Organizing committee

Barry C. Buckland  
Richard V. Calabrese  
Lionel Choplin  
Arthur W. Etchells  
Donald J. Koestler  
Michael B. Lakin  
Gloria Miller  
Alvin W. Nienow  
Gary B. Tatterson

Merck & Co.  
University of Maryland  
University of Laval  
E.I. du Pont de Nemours & Co.  
Rohm and Haas Co.  
Hoechst Celanese Corp.  
Rohm and Haas Co.  
University of Birmingham  
North Carolina A&T State University

#### Officers of the North American Mixing Forum, 1989 to 1992

President: James Y Oldshue  
Vice President: E. Bruce Nauman  
Treasurer: Richard V. Calabrese  
Secretary: Piero M. Armenante

# Index

## A

Aerated stirred tank reactors....98  
Air entrainment.....119

## B

Bubble spectra.....119  
Buoyant particles, mixing....55

## C

Chaotic heat and mass transfer....44  
Closure.....83  
Coalescence, effects on....60  
Cooling coils, helical.....11

## D

Dispersions, liquid-liquid.....60  
Distribution, residence time.....88  
Drop charge effects, investigation of.....60

## F

Filamentous suspensions.....114  
Fluids, mixing of non-Newtonian ...33  
Fluidic mixers.....50  
Fokker-Planck molecular mixing.....83

## G

Gasphase motion, structure of.....98

## H

Heat transfer, multiphase local.....93

Heat and mass transfer, chaotic....44  
Helical ribbon impeller.....28,33

## L

Liquid jets, at acute angles.....119  
Liquid-liquid dispersions, agitated....60

## M

Mass transfer, chaotic....44  
Micromixing efficiency.....6  
Mixers  
    fluidic.....50  
    tee.....23  
Mixing  
    imperfect.....1  
    effect of helical cooling coils on....11  
    experimental mixing data.....18  
    fluidic mixers.....50  
    in a large storage tank.....77  
    molecular.....83  
    non-Newtonian viscous fluids.....33  
    shear-thinning behavior on.....28  
    scale-up procedures ....38  
    storage tanks.....77  
    technology.....55  
    tee.....23  
    vessel.....93

## N

Non-Newtonian fluids.....28, 33, 38  
Non-reactive and reactive flows....23  
Non-standard vessel.....55

## O

Off-bottom distance, effect of.....72

Oxygen transfer, characterization of....114

## P

Paddle design, effect of.....88  
Parallel competing reactions, use of.....6  
PDF modeling.....83  
Plunging liquid jets.....119  
Polycondensation reactors.....18  
Power calculation in mixing.....38  
Precipitate particle size, control of....50  
Product distributions.....1  
Procedures, scale-up.....38

## R

Reactor(s)  
    multiphase.....103, 109  
    polycondensation, melt phase....18  
    sparged, phenomena in.....103  
    stirred semi-batch.....1  
    stirred tank.....98  
    systems, two-phase liquid, liquid....11  
    tee.....23  
Residence time distribution.....88  
Ribbon impeller, helical.....28

## S

Scale-up procedures.....38  
Shear-thinning behavior, effect of.....28  
Solid suspension.....72  
Sound production.....103  
Sparged reactors.....103, 109  
Stirred semi-batch reactor.....1  
Stirred tank reactors.....98  
Stirred tube, distribution in a.....88  
Storage tank, mixing in.....77  
Submergence of solids.....55

## T

Tank, storage.....77  
Tees and jets, area production in.....65  
Tee mixers, design of.....23  
Three-dimensional numerical studies....33  
Turbulent flows.....83

## V

Vessel, non-standard.....55  
Viscosity, effect of paddle design ..88.  
Viscous fluids.....33



## CONTENTS

FOREWORD .....	iii
<u>REACTING SYSTEMS</u>	
IMPERFECT MIXING AND PARADOXICAL PRODUCT DISTRIBUTIONS FOR A STIRRED SEMI-BATCH REACTOR .....	R. Mann and A.M. El-Hamouz 1
USE OF PARALLEL COMPETING REACTIONS TO CHARACTERIZE MICROMIXING EFFICIENCY .....	Jacques Villiermaux, Laurent Falk, Marie-Christine Fournier and Claude Detrez 6
EFFECT OF HELICAL COOLING COILS ON MIXING IN TWO PHASE LIQUID-LIQUID REACTOR SYSTEMS .....	Sunil Satija and David A. Pierce 11
MODELING HIGH VISCOSITY MELT PHASE POLYCONDENSATION REACTORS USING DIRECT INCLUSION OF EXPERIMENTAL MIXING DATA .....	Swati Neogi and Kendree J. Sampson 18
DESIGN OF TEE MIXERS FOR NON-REACTIVE AND REACTIVE FLOWS .....	L.J. Forney 23
<u>VISCOUS SYSTEMS</u>	
ON THE EFFECT OF SHEAR-THINNING BEHAVIOR ON MIXING WITH A HELICAL RIBBON IMPELLER .....	E. Brito de la Fuente, J.C. Leuliet, L. Choplin and P.A. Tanguy 28
MIXING OF NON-NEWTONIAN VISCOUS FLUIDS WITH HELICAL IMPELLERS: EXPERIMENTAL AND THREE-DIMENSIONAL NUMERICAL STUDIES .....	P.A. Tanguy, R. Lacroix, F. Bertrand, L. Choplin and E. Brito de la Fuente 33
SCALE-UP PROCEDURES FOR POWER CALCULATION IN MIXING OF NON-NEWTONIAN LIQUIDS .....	Peter Forschner, Rainer Krebs, Torsten Schneider, Len Kaplan and Gene Smith 38
APPLICATIONS OF CHAOTIC HEAT AND MASS TRANSFER ENHANCEMENT .....	N. Acharya, M. Sen and H.-C. Chang 44
<u>PARTICLE AND LIQUID LIQUID SYSTEMS</u>	
THE CONTROL OF PRECIPITATE PARTICLE SIZE USING FLUIDIC MIXERS .....	J.W. Stairmand, L.H. Ford and M.J. Bowe 50
MIXING TECHNOLOGY FOR BUOYANT PARTICLES IN A NON-STANDARD VESSEL .....	Habib Siddiqui, George Gwilliam and Ramon Perez 55
AN INVESTIGATION OF DROP CHARGE EFFECTS ON COALESCENCE IN AGITATED LIQUID-LIQUID DISPERSIONS .....	T. Tobin, D. Ramkrishna and R. Muralidhar 60
INTERFACIAL AREA PRODUCTION IN TEES AND JETS .....	Richard T. Long, Jr., Israel Tavarez, Wei Lin and Paul Reimus 65
THE EFFECT OF OFF-BOTTOM DISTANCE OF AN IMPELLER FOR THE "JUST SUSPENDED SPEED" $N_{js}$ .....	J.Y. Oldshue and R.N. Sharma 72
<u>TURBULENT MIXING</u>	
MIXING IN A LARGE STORAGE TANK .....	Peter D. Hoffman 77
THE FOKKER-PLANCK MOLECULAR MIXING CLOSURE FOR PDF MODELING OF TURBULENT FLOWS .....	Rodney O. Fox 83
EFFECT OF PADDLE DESIGN AND VISCOSITY ON THE RESIDENCE TIME DISTRIBUTION IN A STIRRED TUBE .....	Guotai Zhang, Timothy J. Diekmann and Gerd Renno 88
<u>HEAT TRANSFER AND GAS LIQUID SYSTEMS</u>	
MULTIPHASE LOCAL HEAT TRANSFER IN A MIXING VESSEL .....	Seung Joo Haam, Robert S. Brodkey and Julian B. Fasano 93



STRUCTURE OF THE GASPHASE MOTION IN AERATED STIRRED TANK REACTORS .....	J. Fischer, S. Broring and A. Lubbert	98
EXPERIMENT STUDIES OF INTERFACIAL PHENOMENA IN SPARGED REACTORS .....	Larry A. Glasgow, Jiaming Hua, Tian-yih Yiin and L.E. Erickson	103
MEASURING TECHNIQUES TO CHARACTERIZE MULTIPHASE REACTORS .....	S. Bodmeier, W. Claas and A. Lubbert	109
CHARACTERIZATION OF OXYGEN TRANSFER IN FILAMENTOUS SUSPENSIONS .....	C. Kurt Suhl and Thomas R. Hanley	114
AIR-ENTRAINMENT AND BUBBLE SPECTRA OF PLUNGING LIQUID JETS AT ACUTE ANGLES .....	Richard M. Detsch, Teresa Stone, and Rajendra N. Sharma	119
INDEX .....		126

# IMPERFECT MIXING AND PARADOXICAL PRODUCT DISTRIBUTIONS FOR A STIRRED SEMI-BATCH REACTOR

R. Mann and A.M. El-Hamouz ■ University of Manchester Institute of Science and Technology, (UMIST), Manchester, England

For a triplet consecutive halogenation sequence forming mono-, di- and tri-substituted products, under perfect mixing there would be no effect of addition time. Also under perfect mixing, the final tri-product can only appear after the first and second products are formed. Imperfect mixing violates both these qualitative features. The quantification of imperfect mixing has been achieved using the network-of-zones model for a typical 30 dm<sup>3</sup> semi-tech stirred vessel being stirred at 100 rpm. For equal rate constants for each of the triplet sequence



it is demonstrated that addition times between 40 and 200 seconds cause a reversal of product appearance from the perfect mixing case, so that the tri-product appears ahead of both the mono- and di-products or else ahead of just the di-product. The corresponding concentration fields of the substituting halogen B during semi-batch operation are presented as sectional image reconstructions - localized concentrations of B emanating from the point of addition cause the paradoxical reversal of the product sequence. The calculations presented are relevant to industrial halogenations of hydrocarbons which involve miscible liquid mixing.

**Introduction** Perfect mixing is often assumed in the assessment and description of stirred vessel chemical reactors. It is frequently the case, however, that the assumption remains untested. In practice, the validity of assumed perfect mixing requires an assessment of the interactions of the rates of chemical reactions with the rates of mixing induced by stirring. Mixing by stirring results from the action of convective flow plus any associated turbulence. Applications of the network-of-zones model has progressed from flow follower simulations (1), through description of tracer dispersal and mixing (2,3), to most recent work on pairs of reactions (4,5) which exhibit significant partial segregation. The network-of-zones model has also been shown to be useful in predicting gas dispersion for a stirred gas-liquid reactor (6) and describing axial and radial solids concentration gradients in single (7) and multiple (8) impeller vessels. In this work we examine the effects of imperfect mixing for a triplet set of reactions, using a network-of-zones formulation for a stirred reactor fitted with a radial flow Rushton impeller.

**Three Reactions Under Perfect Mixing** Before considering the impact of departures from the ideal of perfect mixing, it is appropriate to briefly present the formulation of the perfect mixing equations for a triplet sequence of competitive/consecutive reactions. In line with typical halogenation sequences for hydrocarbons, the reaction scheme under consideration is generally written  $A+B \rightarrow AB+B \rightarrow AB_2+B \rightarrow AB_3$  or  $A+B \rightarrow R+B \rightarrow S+B \rightarrow T$ .

Under perfect mixing with simple mass action type

kinetics, the kinetic rate equations when integrated yield the concentration trajectories of the five components. Of particular interest for practical batch processing is the instantaneous fractional yield of a product I with respect to reagent A denoted by  $\varphi$ . For the initial product R this is given by

$$\varphi\left(\frac{R}{A}\right) = \frac{k_1 C_A C_B - k_2 C_R C_B}{k_1 C_A C_B} = 1 - \frac{k_2 C_R}{k_1 C_A} \quad (1)$$

so that the relative yield of product R is independent of the concentration of B. This means that the relative yield of R and the other products S and T are quite independent of the rate of addition of reagent B under semi-batch operation where B is added to A.

By way of illustration, we shall examine the behaviour of an isothermal semi-tech reactor of volume 30 dm<sup>3</sup> stirred by a Rushton turbine at 100 rpm. The results for a semi-batch addition of B over 200 seconds are shown in Fig.1 where the charge of B is three times the initial molar charge of A, so that the reaction will proceed through to complete reaction to the final product T. With  $k_1 = k_2 = k_3 = 500 \text{ m}^3 \text{ kmol}^{-1} \text{ s}^{-1}$ , the concentration trajectory of A shows an approximately first order disappearance. The first product R reaches a dimensionless maximum at 0.36 after about 70 seconds and the second product S peaks at 0.28 after some 130 seconds. The final product T accumulates progressively at an accelerating rate up to an inflexion point at around 190 seconds. In line with the use of equal rate constants, the final product T only begins to appear at an appreciable level after the primary and secondary products have passed

sequentially through their maximum values. The result of the independence of  $\varphi$  upon the concentration of B as shown in Eqn.1, suggests that there could be no interest in the variation of the rate of addition of reagent B. This is only true, however, provided that the assumption of perfect mixing is reasonably valid. In order to predict the effects of the interactions of internal mixing and addition rate of B upon this triplet sequence of reactions, it is necessary to set up a valid model of the interactions which can account for the finite rates of mixing, flow and reaction which are present in real cases.

**Formulation of a Network-of-Zones Analysis** Fig.2 shows a modified form of the previous network-of-zones (2,3) which accommodates the impeller at a clearance above the base of  $c = H/3$ . For this one third clearance positioning, there is an  $N \times N$  set of zones below the impeller and a set of  $N \times 2N$  zones above the impeller. There are then  $N/2$  concentrically nested flow loops below the impeller as well as above it. Fig.2 shows the two innermost flow loops around each of the upper and lower foci of circulation. In Fig.2 the outermost flow loops above and below the impeller are shown partially complete, indicative of the general case for arbitrary  $N$  values. It is possible to introduce any form of internal velocity profile by allocating the overall impeller generated flow equally amongst the flow loops (totalling  $N$ ) and adjusting the set of zone volumes accordingly. However, earlier work (2) showed that such volume manipulation to adjust the velocity profiles made almost no difference to the mixing behaviour when compared with the simple equal volume case. This is equivalent to the mixing being dominated by the overall convection rate of the impeller. With  $N = 20$ , the set of zones comprises 1200 zones in total. Each backmixed zone experiences an equal and opposite exchange flow with adjacent zones in adjacent loops. The exchange flows are always 'orthogonal' to the mean circulatory flow and conceptually are meant to simulate the effect of turbulence acting to create mixing between parallel flowing convection streams.

**Semi-Batch Addition of Reagent B** In line with earlier discussions, the vessel is envisaged to hold an initial charge of reagent A and B will be added in concentrated form semi-batchwise over an addition time period  $t_a$ . For an arbitrary  $i, j$  zone, such as the zone (3,  $N + 2$ ) shown ringed in Fig.3, in which the convective flow in a loop is outward (in the direction of increasing  $i$ ), an unsteady material balance for a component  $I$  gives

$$\frac{dC_{I,i,j}}{dt} = \frac{q}{V_{i,j}} \left[ C_{I,i-1,j} - (1+2\beta)C_{I,i,j} + \beta(C_{I,i,j+1} + C_{I,i,j-1}) \right] + r_{I,i,j} \quad (2)$$

Eqn.2 applies to every component in every zone, except for the zone which is the addition point for B. For a linear addition rate of B given by  $q_B^f$  the input term for B is given by the product  $C_B^f q_B^f$ , over the addition period  $t_a$ .

The initial conditions are  $C_{A,i,j} = C_A^0$  and  $C_{B,i,j}, C_{R,i,j}, C_{S,i,j}, C_{T,i,j} = 0$

The set of equations (2) for all  $i, j$  and  $I = A, B, R, S$  and  $T$  can be integrated using any convenient integration routine. For the case of  $N = 20$ , this triplet sequence of reactions requires the solution of 6000 first order ordinary differential equations (odes).

**Imperfect Mixing with Slow Addition of B** A range of simulations will now be examined which have the time of addition  $t_a$  as the principal variable, starting with  $t_a = 200s$ . This provides a direct comparison with the perfect mixing case previously outlined. The overall flow rate generated by the impeller at a stirrer speed of 100 rpm will be obtained from  $Q = 2.75 nD^3$  as suggested by Oldshue (9) and in the present calculations it will be assumed that this overall flow is allocated  $2/3$  to the upper circulation and  $1/3$  to the lower circulation. As a result, the average circulation times are identical above and below the impeller. A network configuration of  $(20 \times 20) + (20 \times 40)$  will be adopted with a turbulent exchange parameter value of  $\beta = 0.2$ , except for the impeller zones where a value of  $\beta = 10$  is used, in line with previous simulations of tracer mixing behaviour.

In constructing sectional concentration fields, a simple linear horizontal shading convention for each zone will be applied (4,5). Fig.3 then shows the computed concentration fields for B over five time intervals from the initial condition to the completion of addition of B semi-batchwise. After 40s, when one fifth of the B has been added, B is only detectable at a concentration greater than  $0.1 C_A^0$  in 3 zones with a maximum of three lines in the addition zone ( $i^*, j^* = 1, 58$ ) just below the liquid surface where  $C_B/C_{A0} \leq 0.7$  but  $> 0.5$ . By the time four-fifths of the B has been added at 160s, the cloud of B, or reagent plume as it appears by shading, has enlarged over about 15 zones. On completion of addition at 200s, there is a large distinguishable plume of B which extends as far as the impeller. The highest concentration at this point extends over two zones just below the addition point. Mixing and reaction continue on cessation of addition, but after a further 10s (equal to 2.2 interval turnovers of the batch fluid), no shading is present on the final sectional image. There is a corresponding evolution of a counterpart concentration field for the primary reagent A throughout the semi-batch addition. The set of image reconstructions for A, using the same shading convention, are set out in the same way as for

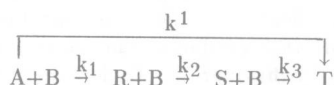


B in Fig.3. The reagent A initially fills the whole vessel at its initial concentration, with every zone shaded with 5 horizontal lines. Over the first 100s or so, the non-uniformity of reagent A is more pronounced than for reagent B. This is because A is continually swept through the zones close to the addition point by convective flow. A is reacted and then convected on towards the impeller. The concentration field of A shows a developing depletion, whilst B forms a smaller pseudo stationary flame or plume which is initially just confined to a few zones below the injection point. This pattern reverses itself however during the second half of the addition. The plume of reagent B continues to grow whilst the zones relatively depleted in A shrink.

The overall effect of the spatially non-uniform concentrations then shows up in Fig.5 which plots the product distribution versus the conversion of A. As Fig.5 shows, the overall effect of the 'real' mixing is to shift the maximum in R significantly lower to a dimensionless value of 0.25. Similarly the dimensionless peak value of S is reduced to about 0.20 but with only a small displacement to a later time. The overall average concentration for the tri-product T is increased at all times except at the very end of the reaction. It is clear from Fig.5 that under this degree of imperfect mixing, the sequence whereby the primary product appears initially, followed by the second product and thereafter the third product is exactly in line with the qualitative behaviour for the initial sequential appearance of mono-, di- and tri-products expected from perfect mixing. Results in Fig.5, use conversion of A as the abscissa.

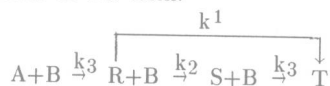
**Imperfect Mixing with More Rapid Addition of B** If the time of addition of B is shortened to 40s, it can be anticipated that a relatively more intense cloud or plume of B will be seen. Details of the concentration field of B, whilst all other conditions are maintained, at the point at which all the B has been added, are shown in Fig.4(b). The detectable field of B delineated by the single shading of zones is always several times larger than for the slower 200s addition case. The behaviour of the concentration field of B is complemented by a correspondingly more severe local depletion of reagent A. There is now more intensive partial segregation of B. The overall result in terms of the integrated average concentration of each component is then shown in Fig.6. It is immediately obvious that the sequence of appearance of each product has now reversed when compared with the result for slower addition in Fig.5. The tri-product T now accumulates in the batch in advance of the mono- and di-products. This is an apparent paradox since it appears as if the tri-product is produced by chemical reaction faster than the initial mono- product. Such behaviour is impossible under perfect mixing unless one presupposes that some hypothetical fast reaction to the final product were to somehow by-pass, by a parallel

path, the normal progressive sequence of product formation. The kinetic scheme would need to have the appearance:



such that the triplet addition or substitution were instantaneous. The resolution of the paradox is of course already obvious from the concentration field in Fig.4(b). The much more intense concentration of B below the point of addition causes the sequence of reactions to advance locally almost to completion to the final product, so that its integrated average rate of appearance (over the whole vessel) is in excess of the overall rates to R and S.

At an addition time of 80s, the behaviour of the concentration field of B as shown in Fig.4(c), lies intermediately between those shown in Fig.4(b) at 40s and Fig.4(a) at 200s. On completion of addition of B after 80s, the plume of added B still stretches through the impeller, but the greatest concentration of B now only extends part way down to the impeller itself. There is no multiple shading of zones beyond the impeller tip in this case, so that the 'visible' plume extending beyond the impeller is much less concentrated. The intermediate behaviour of the overall averaged concentrations is then shown in Fig.7. Product R and product S appear with maxima as in each of the other two cases. However, it is now the case that the tri-product T accumulates after the initial appearance of R but in advance of the accumulation of S. On a simplistic basis, with assumed perfect mixing, this case has apparent reaction kinetics of the form:



with T seemingly formed directly by a 'shunt' from R. As before, the explanation arises from localised over-reaction as a result of a locally high concentration of B. It is obvious that imperfect mixing gives rise to a whole range of possible distortions of the product distribution, some of which can appear paradoxical with reference to perfect mixing.

### Conclusions

The network-of-zones model can be applied to evaluate the effect of imperfect mixing on the triplet sequence of reactions



for semi-batch addition of B to a stirred vessel charged with reagent A. For a  $(20 \times 20) + (20 \times 40)$  division of the reactor volume, a representative set of parameters shows how the degree of partial segregation of the reagents A and B is affected by linear time of

addition (effectively addition rate). The partial segregation of A and B can be conveniently visualised using a simple degree of shading for each zone in the network, providing for a sectional image reconstruction of the concentration field. The concentration trajectories of each of the products can show an apparently paradoxical behaviour. Under perfect mixing, the primary product must appear initially ahead of the second product, which is then followed by the final product. For very strong segregation of A and B, caused by a rapid addition of B, it is shown that it is possible for the final product to appear initially well ahead of the first and second products, even though in passing through maxima, the primary and secondary products show a behaviour in accordance with simple chemical kinetics. With sufficiently slow addition, the behaviour of product trajectories is qualitatively close to that expected for perfect mixing. At an intermediate rate of addition of B, an attenuated paradox can be observed, whereby the final product appears after the first one, but ahead of the second one.

#### Nomenclature

$C_I$	concentration of component I
$c$	impeller clearance
$D$	impeller diameter
$H$	liquid depth
$i$	radial zone position
$j$	axial zone position
$k_{1,2,3}$	reaction rate constants
$N$	network size
$n$	impeller rotation speed
$Q$	total internal flow rate
$q$	zone loop flow rate
$r_I$	reaction rate
$T$	tank diameter
$t$	time
$V_{i,j}$	zone volume
$\varphi(I/A)$	instantaneous yield of product I
$\beta$	turbulent exchange flow ratio
$\Phi(I/A)$	overall yield of product I

#### Literature Cited

1. Mann, R., Mavros, P. and Middleton, J.C., 1981, "A Structured Stochastic Flow Model for Interpreting Flow Follower Data from a Stirred Vessel", *Trans. I.Chem.E.*, **59**, 271
2. Mann, R. and Knysh, P., 1984, "Utility of Interconnected Networks of Backmixed Zones to represent Mixing in a Closed Stirred Vessel", *I.Chem.E. Symp. Series*, **89**, 127
3. Mann, R., Knysh, P., Rasekoala, E.A. and Didari, M., 1987, "Mixing of a Tracer in a Closed Stirred Vessel: A Network of Zones Analysis of Mixing Curves Acquired by Fibre Optic Photometry", *I.Chem.E. Symp. Series*, **108**, 55
4. Mann, R. and Wang, Y.D., 1990 "Mixing in a Stirred Semi-Batch Reactor: Partial Segregation

for a Pair of Reactions Analysed via Networks of Zones", *I.Chem.E. Symp. Series*, **121**, 241

5. Mann, R. and El-Hamouz, A.M., 1991, "Effect of Macromixing on a Competitive/Consecutive Reaction in a Semi-Batch Stirred Vessel", *Proc. 7th European Conf. on Mixing, Bruges*, (in press)
6. Mann, R. and Hackett, L.A., 1988, "Fundamentals of Gas-Liquid Mixing in a Stirred Vessel: An Analysis Based on Networks-of-Zones", *Proc. 6th Europe Conf. Mixing*, 321
7. Brucato, A. and Rizzuti, L., 1988, "The Application of the Networks-of-Zones Model to Solid-Liquid Suspension", *Proc. 6th European Conf. on Mixing*, 273
8. Brucato, A., Magelli, F., Nocentini, M. and Rizzuti, L., 1991, "An Application of the Network-of-Zones Model to Solids Suspension in Multiple Impeller Mixers", *Trans. I.Chem.E.*, **69** (Part A), 43
9. Oldshue, J.Y., 1983, "Fluid Mixing Technology", p174, McGraw-Hill

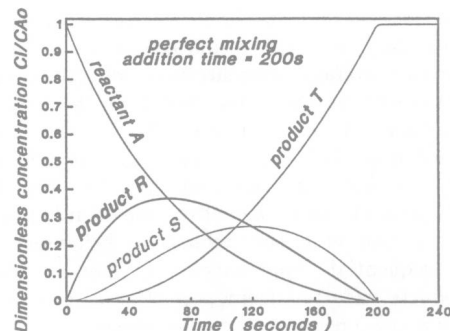


FIG.1 : Reaction Trajectories for Perfect Mixing

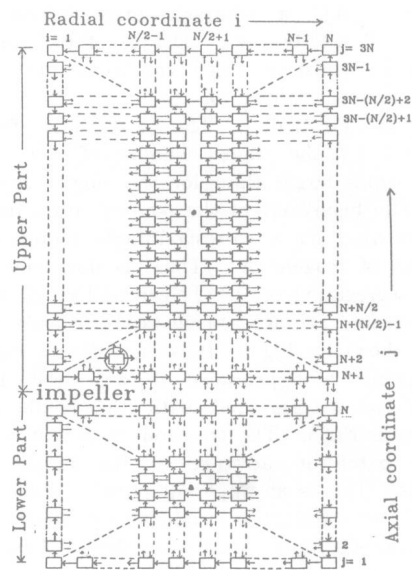


FIG.2 : Schematic Arrangement for Network-of-Zones

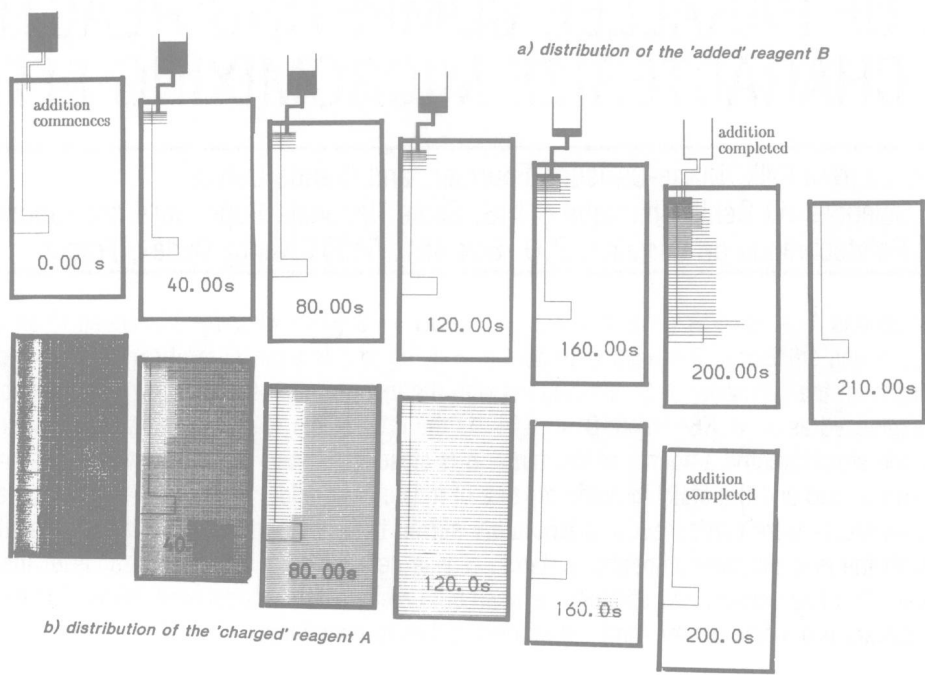


FIG. 3 : Concentration Fields of Reagents for 200s Addition of B

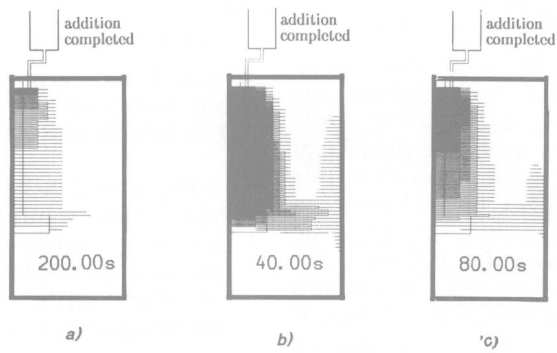


FIG. 4 : Partial Segregation of the "added" reagent B

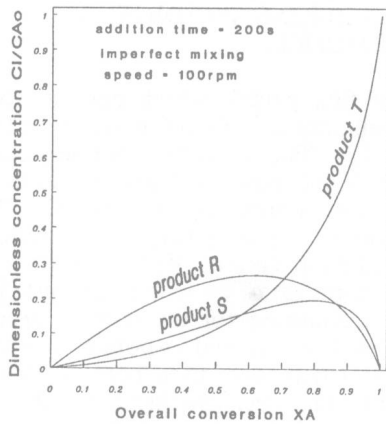


FIG. 5 : Network-of-Zones Prediction for 200s Addition of B

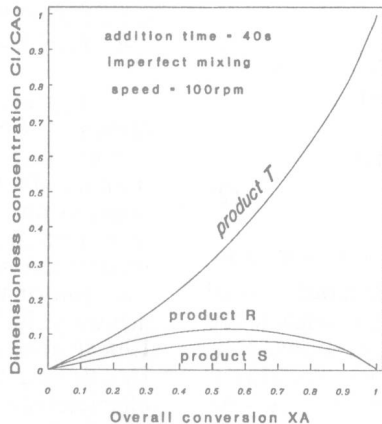


FIG. 6 : Network-of-Zones Prediction for 40s Addition of B

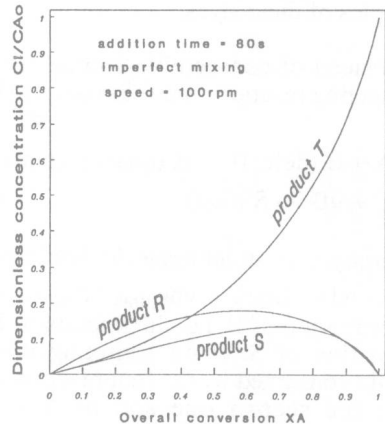


FIG. 7 : Network-of-Zones Prediction for 80s Addition of B



# USE OF PARALLEL COMPETING REACTIONS TO CHARACTERIZE MICROMIXING EFFICIENCY

Jacques Villiermaux, Laurent Falk, Marie-Christine Fournier, and Claude Detrez

■ Laboratoire des Sciences du Génie Chimique CNRS, Ecole Nationale Supérieure des Industries Chimiques, Institut National Polytechnique de Lorraine, P.O. Box 451, 54001 Nancy Cedex, France

Parallel-competing reactions  $A + B \rightarrow R$  (instantaneous),  $C + \nu B \rightarrow S$  (fast) whereby B is added to an excess of A + C may be used to assess micromixing efficiency. The relative amount of B going to S is a measure of segregation intensity. A segregation index  $X_S$  may be defined from the selectivity of S. Simulations with the Incorporation Model show that the micromixedness ratio  $\alpha = (1 - X_S)/X_S$  may be expressed as  $\alpha = KB^n$  where  $B = t_{R2}/t_m$  is the ratio of the reaction time  $t_{R2}$  to the micromixing time  $t_m$ . K and n depend both on the stoichiometric amounts of reactants. n is close to 1 when B is large. A new system is proposed where A is a weak acid, B a strong acid and C a stoichiometric mixture of iodate and iodide. S is iodine which can be easily measured by spectrophotometry. Experiments were carried out in a laboratory stirred tank both with the standard consecutive-competing diazo reaction system and with the new parallel-competing systems.  $\alpha$  was determined at various locations of the injection point as a function of stirring speed. Good agreement was obtained between both methods and model predictions. The new parallel-competing reaction system thus appears promising for micromixing studies in mixing equipment.

Experimental test reactions giving products whose selectivity is significantly dependent on micromixing are useful to validate scale-up procedures of industrial mixers and to assess mixing efficiency. Consecutive competing reactions  $A + B \rightarrow R$ ,  $R + B \rightarrow S$  have been extensively used in this respect. The "Swiss School" has especially developed diazo-coupling reactions where A is 1-naphtol and B diazotized sulfanilic acid. The yield  $X_S$  of S based on B is a segregation index. However, this system presents certain disadvantages, which have been recently pointed out by several authors [3] [4]. The reaction produces in fact two isomers of monazo dye, the para and the ortho form [5], therefore, the definition of  $X_S$  is more complicated. The concentrations of dyes R and S are determined spectrophotometrically and this is a source of inaccuracy especially with respect to the extinction coefficient of S, as it is difficult to isolate pure samples of these dyes.

Instead of consecutive-competing reactions, parallel-competing reactions may also be used [1] [2]



whereby B in stoichiometric defect is added to a mixture of A and C. Let  $Y = \nu n_{S,\max} / n_{B0}$  be the yield of S at total consumption of B, i.e. the fraction of B which leads to the formation of S. If micromixing is instantaneous, B is totally consumed by the first reaction which is much faster than the second one and no S is formed,  $Y_M = 0$ . Conversely, if the fluid is segregated, micromixing is infinitely slow with respect to both reactions which appear

as instantaneous from the standpoint of B. This reactant is thus consumed in the ratio of the concentration of A and C present in the medium. Taking into account the stoichiometric coefficient  $\nu$ , the yield of S is then  $Y_S = \nu n_{C0} / (\nu n_{C0} + n_{A0})$ . A normalized segregation index  $X_S$  may thus be defined as  $X_S = Y/Y_S$ , which varies between 0 for perfect micromixing and 1 for total segregation.

The aim of this paper is to study how  $X_S$  depends on the micromixing time  $t_m$ , to compare the performance of parallel - competing and consecutive - competing reactions, and to present experimental results obtained in a laboratory stirred tank with a new system of parallel-competing reactions.

## SEGREGATION EFFECTS ON PARALLEL-COMPETING REACTIONS PREDICTED BY THE INCORPORATION MODEL.

The principle of this model, which belongs to the family of "Engulfment models" [6], has been presented in a preceding paper [7]. The reacting volume consists initially of a volume  $V_{20}$  containing B and a volume  $V_{10}$  containing the other reactants A and C. Upon micromixing, volume  $V_2$  is assumed to gradually incorporate the fluid from volume  $V_1$  and to grow as a function of time according to  $V_2 = V_{20} g(t)$ ,  $g(t)$  is an arbitrary function accounting for the mixing process. Linear growth  $g(t) = 1 + t/t_m$  and exponential growth functions  $g(t) = \exp(t/t_m)$  were tried here,  $t_m$  being a characteristic micromixing time. The linear growth means that incorporation takes place with a constant flow-rate. The exponential growth corresponds to an incorporation

flow-rate proportional to the volume  $V_2$  of the partially segregated zone. Such a law was used for instance in a model proposed by Zwietering [8]. Mixing is assumed to occur instantaneously within  $V_2$  and the incorporation is thus the controlling process. Chemical reactions are also assumed to occur only in volume  $V_2$ .

The first reaction  $A+B \rightarrow R$  is assumed instantaneous and the rate of the second one  $C+vB \rightarrow S$  is assumed to be  $r_2 = k_2 C_B^\beta C_C^\gamma$ . The mass balance equations in reduced form are easily derived as follows

$$\begin{cases} \frac{d\varphi_B}{d\theta} = -(P+\varphi_B) \frac{d \ln(g)}{d\theta} - v \frac{\varphi_B^\beta \varphi_C^\gamma}{B} & (3) \\ \frac{d\varphi_C}{d\theta} = (Q-\varphi_C) \frac{d \ln(g)}{d\theta} - \frac{\varphi_B^\beta \varphi_C^\gamma}{B} & (4) \\ \frac{d\varphi_S}{d\theta} = -\varphi_S \frac{d \ln(g)}{d\theta} + \frac{\varphi_B^\beta \varphi_C^\gamma}{B} & (5) \\ \theta = 0, \varphi_B = 1, \varphi_C = \varphi_S = 0 & (6) \end{cases}$$

The reduced variables are  $\theta = t/t_m$ ,  $\varphi_B = C_B/C_{B0}'$ ,  $\varphi_C = C_C/C_{C0}'$ ,  $\varphi_S = C_S/C_{S0}'$ ,  $P = C_{A0}'/C_{B0}'$ ,  $Q = C_{C0}'/C_{B0}'$ ,

$$B = t_{R2}/t_m = \left( k_2 C_{B0}'^{\gamma+\beta-1} t_m \right)^{-1}$$

where

$$C_{B0}' = n_{B0}/V_{20}, C_{C0}' = n_{C0}/V_{10}, C_{A0}' = n_{A0}/V_{10},$$

$$C_B = n_B/V_2, C_C = n_C/V_2, C_S = n_S/V_2.$$

Knowing the mixing function  $g(\theta)$ , the system (3) to (6) is easily integrated until total consumption of B i.e.  $\varphi_B=0$  corresponding to  $g_{\max} = 1 + (P+vQ)^{-1}$ . The final yield of S is  $Y = v\varphi_{S, \max} g_{\max}$  and the segregation index is  $X_S = Y/Y_S$  where  $Y_S = vQ/(P+vQ)$

It is interesting to consider the quantity  $\alpha = (1-X_S)/X_S = (Y_S/Y) - 1$  that we have named the "micro-mixedness ratio" [9]. It has been shown with other systems [7][10] that  $\alpha$  is proportional to  $B = t_R/t_m$  for sufficiently large values of B. Figure 1 confirms this fact from numerical simulations performed with  $\beta=2, \gamma=2, v=2$  and various values of P, Q with the two incorporation laws. The linear relationship  $\alpha = KB$  is observed only for

$B > 1$ . However, the proportionality constant K depends mainly on the stoichiometric ratio  $Q/P$ . In the region  $B \ll 1$ , the slope of  $\alpha$  vs. B in log-log plot is smaller. Numerical simulations performed with  $P = 0.02225$  and  $Q = 0.00175$  corresponding to the experimental conditions which were used for experiments presented below show that for  $B < 10^{-5}$ ,  $\alpha$  varies as  $B^m$  with m of the order of 0.3. This remark will be useful for the interpretation of experimental data.

Similar results may be obtained by the Diffusion Model where it is assumed that upon injection of B into the A,C mixture, small aggregates of B are produced which later mix by simultaneous diffusion and chemical reaction. It was shown in reference [10] that diffusional and lumped mixing models (e.g. the IEM model) yield equivalent results for predicting the influence of segregation on chemical reactions if their characteristic micromixing times are equal. For aggregates of thickness  $2\delta$ , the diffusion time is  $t_D = \delta^2 / [(p+1)(p+3)D]$  where p is a shape factor,  $p = 0$  for slabs,  $p = 1$  for long cylinders and  $p = 2$  for spheres [12]. Setting  $t_D = t_m$ , one obtains the equivalence condition between Diffusion and Incorporation models  $B = (p+1)(p+2) / Da_2$  where  $Da_2 = k_2 C_{B0}'^{\beta+\gamma-1} \delta^2 / D$ .

Figure 2 shows that the results for long cylindrical filaments are close to those of the Incorporation model with a linear growth mixing function.

#### A NEW SYSTEM OF PARALLEL-COMPETING REACTIONS. EXPERIMENTAL STUDY OF MICROMIXING EFFICIENCY IN A LABORATORY STIRRED TANK.

We propose a new system of parallel reactions suitable for micromixing tests. Species B are protons supplied by a strong acid. A is a base  $A^-$  supplied by a weak acid AH. The first reaction is thus a mere neutralization



The second reaction is the iodate-iodide reaction which releases iodine



C denotes the potential amount of iodine  $I_2$  contained in the mixture  $IO_3^- + 5I^-$ , namely  $3I_2$ , therefore, reaction (8) can be written



and the stoichiometric coefficient is  $\nu=2$ . The weak acid AH is selected in such a way that iodine is produced quantitatively according to reaction (8) and the pH remains in a range where the reverse reaction of  $I_2$  dismutation into  $IO_3^-$  and  $I^-$  is slow. The amount of  $I_2$  produced is easily determined by absorption spectrophotometry in the form of  $I_3^-$  at 353 nm. Reaction (7) is a neutralization and may be considered as quasi-instantaneous. Reaction (8) is very fast, and known in the literature as the "Dushman reaction" [13]. Its kinetics is not totally elucidated yet, especially under the conditions of composition and ionic strength used in this study. It has been assumed that  $r_2 = k_2 C_B^2 C_C^2$ , where C is the "potential"  $I_2$  but this expression is probably too simplistic and  $r_2$  should be measured by appropriate methods for a quantitative interpretation of the data presented below aiming at the determination of  $t_m$ .

Experiments were carried out in a standard stirred tank of  $V = 1 \text{ dm}^3$  fitted with four baffles and a six bladed Rushton turbine. The reactor was initially filled with  $880 \text{ cm}^3$  of a solution of A and C. After a homogenization period of 5 minutes, a small amount of B ( $1 \text{ cm}^3$  in the case of concentrated acid) was slowly injected into the tank at various positions 1 cm far from the wall between two baffles. It was checked that the injection time (here about 35 s) had no influence on results, proving that only micromixing phenomena were concerned. After completion of the reaction,  $S = I_2$  was measured by absorption spectrophotometry and  $X_S$  was calculated. The determination of S must be carried out as quickly as possible in order to prevent the reverse dismutation reaction to occur, to a significant extent. The segregation index was measured for several values of the stirring speed  $N$  ranging between 2 and  $50 \text{ s}^{-1}$ . This corresponds to agitation Reynolds numbers comprised between 2700 and 67000.

The set of stoichiometric ratios used were

	(a)	(b)	(c)	(d)	(e)	(f)	(g)
P	$2.225 \times 10^{-2}$	$2.225 \times 10^{-2}$	$3.4 \times 10^{-2}$	0.1125	0.70	1.41	2.83
Q	$1.75 \times 10^{-3}$	$1.75 \times 10^{-2}$	$4.5 \times 10^{-3}$	$2.25 \times 10^{-2}$	0.87	1.75	3.50
$C_{Bo}$	4000*	4000*	2000*	400*	80*	40*	20*

\* in  $\text{mol.m}^{-3}$

The positions of injection in the tank along a vertical line at 1 cm from the wall between two baffles were <1> : 3 cm beneath the surface, <2> : in the turbine discharge, <3> : 3 cm above the bottom.

Experiments were carried out at room temperature. Figure 3, 4 and 5 shows typical results plotted as

$\alpha = (1-X_S)/X_S$  against  $N$ , together with previous results obtained with a standard diazo-system of consecutive reactions [14]. (A, initially in the tank,  $V_{Ao} = 750 \text{ cm}^3$  of 1-naphtol solution at  $C_{Ao} = 1.39 \text{ mol.m}^{-3}$  and  $\text{pH}=10.0$ . B, added slowly ( $15 \text{ cm}^3.\text{min}^{-1}$ ),  $V_{Bo} = 75 \text{ cm}^3$  of diazotised sulfanilic acid solution at  $C_{Bo} = 13.21 \text{ mol.m}^{-3}$ ).

## DISCUSSION

From the inspection of experimental results, several points can be made. The method yields significant values of  $\alpha$ , which are comparable to those obtained by the consecutive system. The variations of  $\alpha$  as a function of stirring speed, position of the injection point, and concentration of reactants are in agreement with qualitative predictions. In particular,  $\alpha$  increases with  $N$ , and it is larger in the discharge flow of the turbine than close to the surface. However the rate of increase of  $\alpha$  with increasing stirring speed is obviously smaller than with the consecutive reaction system, when the stoichiometric ratios  $P = C_{Ao}'/C_{Bo}'$  and  $Q = C_{Co}'/C_{Bo}'$  are small. Under such conditions, it is possible to explore smaller micromixing times.

For the consecutive system (Figure 3), one obtains approximately straight lines of slope 1.5. This can be explained as in the case of consecutive reactions and under the experimental conditions used, the linear relationship between  $\alpha$  and B holds [7]. B varies as the reciprocal of the mixing time  $t_m$  which in turn may be assumed to depend on the square root of the power dissipation  $\epsilon$ . This is true for the Incorporation Model where  $t_m \propto (\nu/\epsilon)^{1/2}$  and for the diffusion model where  $\delta$  is the Kolmogorov microscale  $\delta \propto (\nu^3/\epsilon)^{1/4}$  and  $t_D \propto \delta^2/D$ . Finally, as  $\epsilon \propto N^3$ ,  $\alpha \propto B$ , then  $\alpha \propto N^{1.5}$  and this is the dependency which is observed with the diazo-system.

The experiments with the system of parallel reactions were performed in a broad concentration range. When the acid B was much more concentrated than A and C, parameters P and Q were small. Under these conditions, the simulation predicts that  $\alpha \propto B^n$  with  $n \approx 0.3$ . Therefore, one should find  $\alpha \propto N^{3n/2}$  with  $3n/2 \approx 0.45$ . This slope is indicated in Figure 4 in fair agreement with the general slope of experimental curves. In addition, the mixedness ratio  $\alpha$  increases from injection point <1> to point <3> and <2>, which is reasonable from expected distribution of power dissipation within the tank. Conversely, when larger values of P and Q are used, the slope increases and comes closer to 1.5, in agreement